Biomaterials 35 (2014) 5294–5306

Contents lists available at ScienceDirect

Biomaterials

journal homepage: www.elsevier.com/locate/biomaterials

The synergetic effect of hydrogel stiffness and growth factor on osteogenic differentiation

ShihJye Tan [a], Josephine Y. Fang [a], Zhi Yang [a], Marcel E. Nimni [a], Bo Han [a,b,*]

[a] Division of Plastic and Reconstructive Surgery, Department of Surgery, Keck Medical School, University of Southern California, Los Angeles, CA, USA
[b] Department of Biomedical Engineering, Viterbi School of Engineering, University of Southern California, Los Angeles, CA, USA

ARTICLE INFO

Article history:
Received 24 December 2013
Accepted 21 February 2014
Available online 3 April 2014

Keywords:
Mechanical properties
ECM (extracellular matrix)
BMP-2
Synergetic effect
Osteogenesis
Cell encapsulation

ABSTRACT

Cells respond to various chemical signals as well as environmental aspects of the extracellular matrix (ECM) that may alter cellular structures and functions. Hence, better understanding of the mechanical stimuli of the matrix is essential for creating an adjuvant material that mimics the physiological environment to support cell growth and differentiation, and control the release of the growth factor. In this study, we utilized the property of transglutaminase cross-linked gelatin (TG-Gel), where modification of the mechanical properties of TG-Gel can be easily achieved by tuning the concentration of gelatin. Modifying one or more of the material parameters will result in changes of the cellular responses, including different phenotype-specific gene expressions and functional differentiations. In this study, stiffer TG-Gels itself facilitated focal contact formation and osteogenic differentiation while soft TG-Gel promoted cell proliferation. We also evaluated the interactions between a stimulating factor (i.e. BMP-2) and matrix rigidity on osteogenesis both *in vitro* and *in vivo*. The results presented in this study suggest that the interactions of chemical and physical factors in ECM scaffolds may work synergistically to enhance bone regeneration.

1. Introduction

Natural bone development reflects the significant role of physical stimuli in bone regeneration, which involves continuous turnover of bone extracellular matrix (ECM) and mineralization through bone resorption and formation. Mechanical loading during normal activities such as climbing and walking helps to enhance bone formation and directs the newly formed cells along the local loading direction. Yet, reduced loading during long-term immobilization or microgravity results in bone loss [1]. The healing process of bone fracture due to aging or accidental incidence also demonstrates the importance of mechanical factors, as the bone is subjected to mechanical regulation during regeneration from soft tissues. A stiff fixation minimizes interfragmentary movement, which results in limited callus formation. On the other hand, interfragmentary micromotion during flexible fixation stimulates callus formation and improves the repair process, whereas unstable fixation prevents the fracture from healing [2–4]. The mechanical properties of fixation influence the healing progression in a direct (intramembraneous) and/or an enchondral pattern that aids the process of ossification [5]. Thus, the mechanical signals are as important as chemical signals in the regulation of bone development, remodeling, and regeneration.

Two dimensional (2-D) *in vitro* studies have shown that the regulation of important cellular processes, such as proliferation, differentiation, and apoptosis, is controlled by the mechanical properties and geometry of the cells and their surrounding environment [6–11]. Apart from cellular processes, the microenvironment may control the cell shape and cytoskeletal tension, and may influence cell-matrix and cell–cell interactions [7,12]. Although 2-D *in vitro* studies have identified several important mechanical cues that can manipulate cell fate [12,13], cells present on a coated 2-D surface might not truly reflect their characteristics in a 3-D environment. At the cellular scale, the surrounding fluid and the ECM exert stresses on cells, and the cells may respond to the applied forces through integrin bindings in an omnidirectional manner [14–19]. The number of integrin-ligand bonds formed by a cell with its surroundings, dictates the extent of cell-matrix interactions [20], the ease with which they migrate through it, and the degree of generated intracellular tension [21–24], which are crucial factors

* Corresponding author. University of Southern California, 1333 San Pablo St., BMT 302A, Los Angeles, CA 90089-9112, USA. Tel.: +1 323 442 2242; fax: +1 323 442 5956.
E-mail address: bohan@usc.edu (B. Han).

http://dx.doi.org/10.1016/j.biomaterials.2014.02.040
0142-9612/

during tissue remodeling, morphogenesis, and differentiation, and normal physiological functioning. Since 2-D cell-matrix interactions are bidirectional, and 3-D are omnidirectional, it might not be suitable to extrapolate the effects of biological signaling due to cell-matrix interactions from 2-D experiments [25]. In addition, the variation of mechanical properties of ECM may lead to concentration gradients existing within the 3-D physiological structure, and this phenomenon cannot be achieved in 2-D *in vitro* studies. The differences in rigidity profiles can potentially affect the behaviors of cells in the center of the matrix different from the behaviors of those close to the periphery, because of the dissimilar local concentrations [26]. Therefore, cell responses to the substrate rigidity should be studied or re-examined in a physiologically relevant 3-D microenvironment.

One of the major challenges in the 3-D study of cell responses to substrate rigidity is the lack of suitable substrates. Even though some researchers [27,28] may have identified correlations between the matrix rigidity and cell phenotype in 3-D, many available materials are not suitable for 3-D studies because of the rigidity. A soft material cannot be assembled into a 3-D structure that can support cell survival throughout a long-term study, and a rigid material limits the cell survival and restrains the variation of substrate rigidity. For instance, by using thixotropic polyethylene glycol-silica gel, Pek et al. [27] showed that cell differentiation can be controlled by modulating the matrix stiffness through variations in the concentrations of the nanoparticles. Though physically cross-linked silicate polymer hydrogels have shown attractive biological properties, their applications as scaffold structures for bone regeneration are limited because of their insufficient mechanical properties [29,30]. On the contrary, silk fibroin protein is rather stable and mechanically robust, but the utilization of silk is restrained from elastomeric biomaterial applications because of its inherent tendency to form stiff materials (>1 MPa) as a result of the beta sheet crystal formation [13]. Hence, the development of a 3-D material that can mimic the physiological ECM allows the investigation of cell responses to substrate mechanics, which are independent of both biochemical and transport properties would be a major breakthrough in tissue engineering.

Injectable transglutaminase cross-linked gelatin (TG-Gel) may be one of the ideal alternative materials owing to its mechanical strength required for supporting cell adhesion, survival, and organization during the regeneration process without compromising on the bioactive substances [31]. The matrix stiffness of TG-Gel can be conveniently tuned by controlling the concentration of gelatin. Hence, TG-Gel was adopted in our 3-D study to examine the effects of rigidity on precursor cells. Moreover, chemical milieus are important to the mimic, as the bone formation, maintenance, and regeneration constitute a complex process involving the interactions of many cellular elements *in vivo*, including growth factors, hormones, cytokines, and ECM components [32]. However, the effects of mechanical changes and their interactions with the growth factors have yet to be adequately explored, and the understanding of their influences may provide new insights into the processes of development, disease, and material-cell-based regeneration. Among the osteoinductive growth factors, BMP-2 has been found to be essential for the initialization of bone regeneration [33]. Therefore, we investigated the effects of chemical stimulating factor (i.e. BMP-2) and matrix rigidity on osteogensis in both *in vitro* and *in vivo* models.

2. Methods and materials

2.1. Cell culture

Mouse C2C12 myoblast cells (ATCC, American Type Culture Collection, Manassas, VA) were initially cultured in a growth medium (GM) consisting of high glucose Dulbecco's modified Eagle medium (DMEM, Mediatech, VA) supplemented with 10% (v/v) fetal bovine serum (FBS, Lonza, MD) and 1% (v/v) penicillin-streptomycin (PS, Mediatech, VA) in a humidified atmosphere of 5% CO_2 at 37 °C. The medium was changed every 2–3 days. When the cells reached 70% confluence, they were subcultured using 0.25% trypsin and 0.02% ethylenediaminetetraacetic acid (EDTA) solution.

2.2. Materials and reagents

Unless otherwise stated, all chemicals and reagents were purchased from Sigma–Aldrich (St. Louis, MO). The preparation of microbial transglutaminase (TG) and gelatin gel (Gel) were reported elsewhere [34,35]. Briefly, gelatin Type A 300 Bloom (Sigma Aldrich, MO) was dissolved and autoclaved in distilled water to generate 10% gelatin stock. Then, 10% gelatin stock solution was diluted with phosphate-buffered saline (PBS, 137 mM NaCl, 2.7 mM KCl, 10 mM Na_2HPO_4, and 1.8 mM KH_2PO_4) to produce gels with final concentrations of 3%, 6%, and 9%. TG from *Streptomyces mobaraense* was obtained from Ajinomoto (Tokyo, Japan), and was further purified with SP Sepharose Fast Flow beads (Sigma–Aldrich, MO). The activity of TG was titrated by the o-phthaldialdehyde (OPA) assay using casein as a substrate [36], and the protein concentration was tested by the Bradford method (Bio-Rad, Hercules, CA) [37] utilizing Bovine Serum Albumin (BSA) as a standard. Gel and TG were stored at 4 °C and −80 °C, respectively.

2.3. Mechanical testing

To quantify the rigidity and porosity of the substrate, transglutaminase cross-linked gelatin (TG-Gel) was created by mixing each 100 μL of pre-heated gel solution with 7 μL of TG. The TG-Gel was shaped into cylinders with the height to diameter ratio (L/D) of 1.25 to avoid mechanical failure modes, such as buckling. Furthermore, the TG-Gel containing trapped bubbles was discarded to avoid obtaining irregular mechanical properties.

2.3.1. Yield strength measurement

The Young's modulus or yield strength (E_{modulus} [kPa]) of TG-Gel was measured using the unconfined compression test, where only lateral deformation of the TG-Gel was induced through compression between two plates. The force (F [N]) required to compress the TG-Gel was recorded at every 1 [cm] of deformation to deduce the stress (σ [kPa]) versus strain relationship. The strain (L^*) is defined by equation (1):

$$L^* = \frac{\Delta L}{L} \tag{1}$$

where ΔL denotes the amount of deformation and L represents the initial height of the TG-Gel. The Young's modulus of the TG-Gel was determined from the slope of the stress versus strain graph and by equation (2):

$$E = \frac{\sigma}{L^*} \tag{2}$$

2.3.2. Porosity measurement

The porosity of the fabricated 3-D scaffold was measured using liquid displacement method as described [38]. Briefly, the TG-Gel was immersed in ethanol of a known volume (V_1) contained in a graduated cylinder for 5 min. Ethanol was selected because it could readily penetrate the open pores of the TG-Gel without inducing swelling or shrinkage. The porosity of the scaffold (ε) is calculated by equation (3):

$$\varepsilon(\%) = \frac{V_1 - V_3}{V_2 - V_3} \times 100\% \tag{3}$$

where V_2 corresponds to the total volume of the ethanol-impregnated scaffold along with ethanol, and V_3 denotes the amount of residual ethanol in the cylinder after the removal of ethanol-impregnated TG-Gel.

2.4. In vitro 3-dimensional TG-Gel model

In vitro 3-D TG-Gel-Cell construct was created to evaluate the effects of matrix rigidity on cellular responses. A pre-myoblast C2C12 cell line was selected to study osteogenic differentiation because C2C12 is a pluripotent mesenchymal precursor cell that provides a model system to study the early stage of osteoblast differentiation during bone formation in muscular tissues and its ALP expression is close to the baseline level when the cells are cultured in 2-D environment [31]. The prepared gel was first heated and liquefied at 60 °C in water bath. Then, every 100 μL of the gel solution was evenly mixed with C2C12s at a density of 2×10^6 cells/ml and 5 μL of TG to create the TG-Gel-Cell mixture. Afterwards, 20 μL of the TG-Gel-Cell mixture was seeded into each well of 48-well suspension plates. After incubation for 1 h at 37 °C, 1 mL of growth medium (GM) was added into each well containing the solidified gel through TG chemical cross-linking. The GM was supplemented with 30 ng/ml BMP-2 (R&D Systems, Minneapolis, MN) to determine the effects of BMP-2 on osteogenesis with the aid of TG-Gel with various rigidities.

2.5. Proliferation and cytotoxicity assays

Cell counting was performed to determine the cell growth. The TG-Gel-Cell construct was washed twice with PBS and incubated with 20 units of Type II microbial collagenase (*Worthington, NJ)* for 5 h to release the cells from the construct. The cell sample was collected and counted using a cell counting machine (Beckman Coulter, CA). The viability of C2C12s encapsulated in TG-Gel was assessed using Cell Counting Kit-8 (CCK-8, Dojindo Molecular Technologies, MD) after the TG-Gel-Cell construct was washed twice with PBS and incubated in 500 μL of CCK working solution (CCK-8 stock solution in growth medium, 1:40) for 4 h. Subsequently, 100 μL of the supernatant was transferred into 96-well plates, and the absorbance was measured in a multiplate reader at 450 nm (Molecular Devices, CA). The cell viability was also determined by evaluating the reduction of an MTT tetrazolium component into an insoluble dark purple formazan produced by the mitochondria of the viable cells [39]. MTT stock solution was prepared by dissolving 0.25 g of MTT powder in 50 mL of dH_2O, and then filtered, and stored at 4 °C until use. The sample was washed twice with PBS and subsequently incubated with 500 μL of MTT working solution (filtered MTT stock solution in growth medium, 1:10). The color development was constantly inspected by light microscopy (Nikon, Japan), and images were taken after 30 min of incubation at 37 °C.

2.6. Cell appearance and cell-matrix interactions analysis

Cell morphology and cytoskeleton organization were visualized by F-actin staining. The TG-Gel-Cell construct was rinsed with Tris-buffered saline with 0.05% Tween 20 (TBST, pH 7.4), fixed in 10% neutral formalin solution (VWR International, PA) for 10 min, and incubated in blocking buffer (5% BSA in TBST) for 30 min. Then, 50 μl of Rhodamine 110 Phalloidin (Biotium, CA) was diluted in each 2 mL blocking buffer, and 500 μL of the solution was used to stain each sample. After 2 h incubation at 4 °C, the TG-Gel-Cell construct was counterstained with DAPI (Biotium, CA) for 5 min and visualized under an EVOS fluorescence microscope (Advanced Microscopy Group, WA).

β1-Integrin immunostaining was performed at room temperature to characterize cell-matrix interactions. The cell culture medium was gently removed, and the sample was washed twice with TBST. Subsequently, the TG-Gel-Cell construct was fixed in 10% neutral formalin solution for 10 min, incubated in peroxidase suppressor solution (Thermo Scientific, NH) for 30 min, and then incubated in the blocking buffer (5% BSA in TBST) for 30 min. Next, the sample was incubated in the primary antibody working solution (anti-β1-Integrin polyclonal antibody in blocking buffer, 1:400, Thermo Scientific, NH) overnight, followed by incubation in the secondary antibody working solution (biotinylated anti-rabbit produced in goat in blocking buffer, 1:800, Sigma, MO) for 1 h. To amplify detection signals, the TG-Gel-Cell construct was incubated in SPPU working solution (ultrasensitive streptavidin–peroxidase polymer in blocking buffer, 1:800, Sigma, MO) for 30 min. The color reaction was revealed by incubating the sample in DAB working solution (metal-enhanced substrate solution diluted with stable peroxide buffer, 1:10, Thermo Scientific, NH), and the reaction was stopped by washing the sample with TBST when the desired color was developed (~5 min). Microscopic analysis was performed to examine the anchored cells.

2.7. Osteogenesis analysis

Alkaline phosphatase (ALP) activity and staining were performed to characterize early osteogenesis. ALP activity, which was determined by a biochemical assay based on the conversion of p-nitrophenyl phosphate to p-nitrophenol (pNPP) measured spectrophotometrically at 405 nm [34,40]. Briefly, the TG-Gel-Cell construct was washed twice with PBS and homogenized with buffer solution (0.25% TritonX-100 in PBS). After three freezing–thawing cycles, the cells were released from the TG-Gel by adding 50 μL of 0.25% trypsin and incubation at 37 °C for 4 h. The ALP activity was then quantified using p-NPP as a substrate (Pierce, USA). The absorbance was measured with a multiplate reader (Molecular Devices, CA) after 30 min of incubation at 37 °C. The ALP activity was defined as an arbitrary unit of ALP absorbance that was normalized with the corresponding cell numbers. For ALP staining, the sample was washed and fixed in 10% neutral formalin solution for 10 min. The color reaction was revealed by incubating the sample in 5-bromo-4-chloro-3-indolyl phosphate/nitro blue tetrazolium (BCIP/NBT) working solution prepared by dissolving 1 BCIP/NBT tablet in 10 mL of dH_2O. The reaction was stopped upon the development of the desired color. Microscopic analysis was performed to examine the differentiated cells.

Alizarin red S staining as a late marker of osteogenic-differentiation was performed to determine the degree of calcium deposition, as described elsewhere [41]. Briefly, the TG-Gel-Cell construct was washed twice with distilled water (dH_2O), fixed in 10% neutral formalin for 10 min, and stained with 40 mM alizarin red S (pH 4.2, Sigma, MO) for 30 min. Prior to photography, the stained sample was washed twice with dH_2O to remove nonspecific precipitates. Positive orange-red staining represents calcium deposition by the differentiated cells. Images were captured for the analysis of late-stage osteogenic differentiation. After photography, dH_2O was removed, and the sample was incubated with 500 μl of 10% (w/v) cetylpyridinium chloride for 10 min to release the bound calcium. The supernatant was collected, and absorbance was measured by a multiplate reader (Molecular Devices, CA). The calcium deposition was specified as an arbitrary unit of calcium deposition absorbance that was normalized with the corresponding cell numbers.

2.8. Total RNA extraction and RT-PCR analysis of the gene expression

Total RNA of the C2C12 cells grown in the TG-Gel was extracted using Trizol reagent (Invitrogen, CA) according to the single-step acid–phenol guanidinium extraction method described by Chomczynski and Sacchi [42]. In brief, encapsulated C2C12 cells were cultured in the media with and without supplementation of BMP-2 in petri dishes for predetermined time points (i.e., 5 and 14 days). The sample was collected in 1.5 mL tubes containing 1 mL Trizol reagent. After a thorough homogenization and removal of insoluble substances, the sample was treated with 1-bromo-3-chloropropane. Total RNA was precipitated using chilled ethanol, and the acquired RNA sample was treated with RNase-free water. The RNA concentration was quantified spectrometrically at 260 and 280 nm, and the purity was determined at 230 and 260 nm (Implen GmbH, Germany). Real-time PCR was performed with one-step SYBR green reagents according to the manufacturer's protocol (Bio-Rad, CA). The expression of target genes was normalized according to the GAPDH gene reference by using the ΔΔCt method. The primers (ValueGene Inc, CA) used for amplification are listed in Table 1.

2.9. In vivo overlay model

All animals used in this study were treated by following the protocols approved by the *Institutional Animal Care and Use Committees* (IACUC) of the University of Southern California. Twenty-Four 2-month-old Fischer-344 rats (NCI) were randomly divided into 6 groups according to different gel rigidities of 3%, 6%, and 9% with and without. Transglutaminase cross-linked gelatin (TG-Gel) with and without BMP-2 was created by mixing 100 μL of each pre-heated Gel solution with 5 μL of TG and 0.5 μg of BMP-2. Each animal was infused with 100 μl of TG-Gel subcutaneously injected on top of the parietal bone of the calvaria by using a G-27 needle. All rats were euthanized 28 days after the injection, and their calvarial bones were removed for histological studies. The removed calvarial bones were fixed, decalcified, and sectioned for hematoxylin and eosin staining (H&E).

2.10. Statistical analysis

The sample size used in all *in vitro* studies was four. Statistical differences were determined using ANOVA, followed by a Tukey–Kramer honestly significant difference (HSD) test for pair-wise comparisons (SAS). A statistical significance was accepted at $^{*}p < 0.05$, $^{**}p < 0.01$, and $^{***}p < 0.001$.

3. Results

3.1. Mechanical properties of TG-Gel

The mechanical properties of the TG-Gel were measured and characterized in terms of yield strength and porosity as depicted in Fig. 1. The TG-Gel exhibited variable force versus axial stress profiles with changes in the gel concentration. In general, the yield strength of a TG-Gel increased with an increase in the gelatin concentration, and 9% TG-Gel exhibited the highest yield strength (32.32 ± 1.9 kPa), followed by the 6% (13.51 ± 2.13 kPa) and 3% TG-Gels (1.58 ± 0.42 kPa). On the other hand, the porosity of TG-Gel decreased with an increase in the gelatin concentration, and 3% TG-Gel exhibited the highest porosity (58.38 ± 2.45%), followed by the 6% (34.89 ± 5.68%) and 9% TG-Gels (17.03 ± 6.44%). These results indicate that the control of gelatin concentration could be used to directly manipulate the

Table 1
Primers used to amplify mRNAs encoding mouse GAPDH.

Primer	Sequence (5′–3′)
ALP – F	CTCCAAAAGCTCAACACCAATG
ALP – R	ATTTGTCCATCTCCAGCCG
Osteoblast – F	AAGAGATGGTCACTTCACGC
Osteoblast – R	GCACTGGAGGGTATTTAGGATG
Osteocalcin – F	ACCATCTTTCTGCTCACTCTG
Osteocalcin – R	GTTCACTACCTTATTGCCCTCC
Osteopontin – F	ACGGAGACCATGCAGAGAGC
Osteopontin – R	TTGTGTGCTGGCAGTGAAGG
Col1 – F	CAGCCGCTTCACCTACAGC
Col1 – R	TTTTGTATTCAATCACTGTCTTGCC
GAPDH – F	ATGGGGAAGGTGAAGGTCG
GAPDH – R	TAAAAGCATCCCTGGTGACC

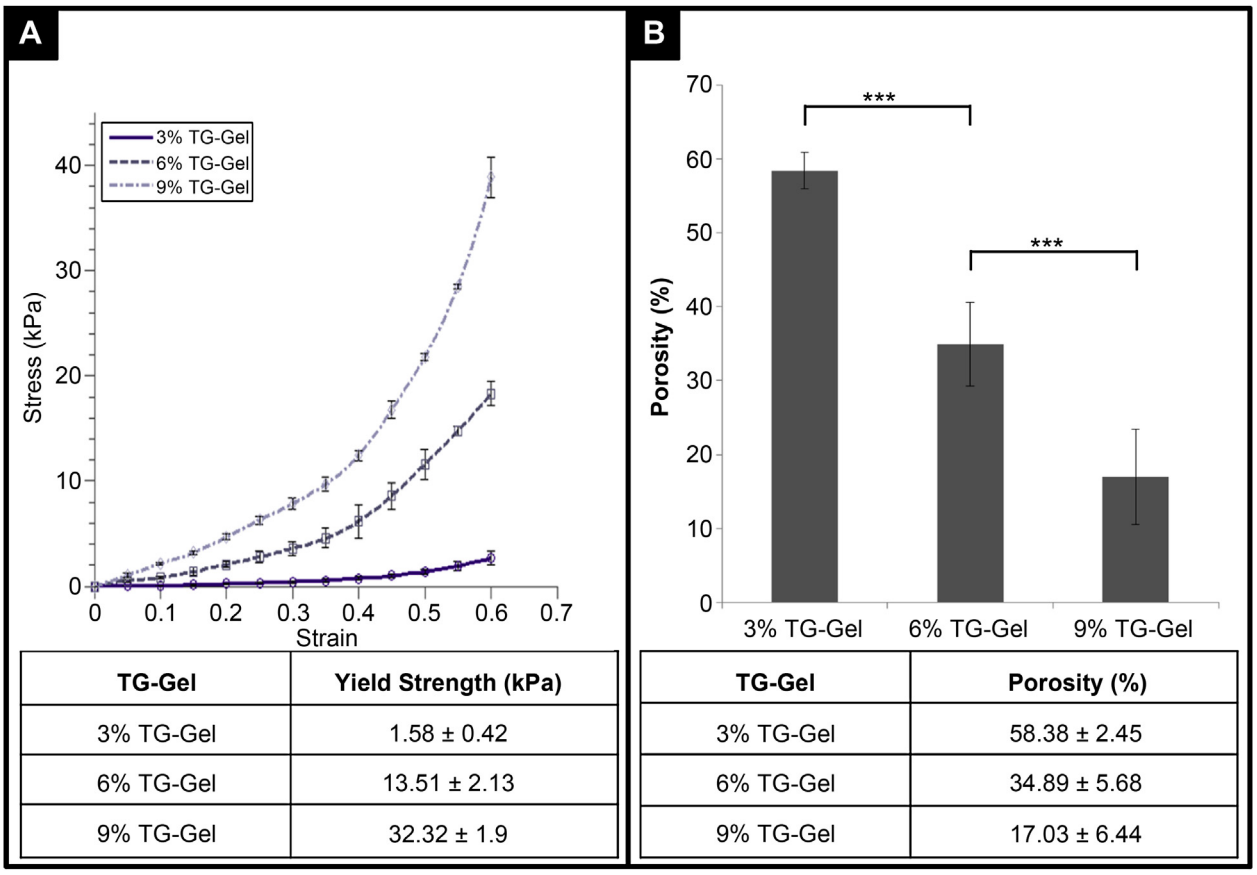

TG-Gel	Yield Strength (kPa)
3% TG-Gel	1.58 ± 0.42
6% TG-Gel	13.51 ± 2.13
9% TG-Gel	32.32 ± 1.9

TG-Gel	Porosity (%)
3% TG-Gel	58.38 ± 2.45
6% TG-Gel	34.89 ± 5.68
9% TG-Gel	17.03 ± 6.44

Fig. 1. Mechanical properties of TG-Gel. (A) Yield strength of a TG-Gel increases with an increase in the gelatin concentration. (B) Porosity of TG-Gel. Porosity of a TG-Gel decreases with an increase in the gelatin concentration. Data are mean ± standard deviation, from 4 samples, statistical differences ($^{*}p < 0.05$; $^{**}p < 0.01$; $^{***}p < 0.001$).

mechanical properties of the insoluble material for assessing the influence of the matrix on cellular responses.

3.2. Cell response to matrix rigidity

Extracellular matrix plays a vital role in transmitting environmental signals to cells, as the environmental signals may affect many aspects of a cell's life such as proliferation and viability [43]. Therefore, cell counting was performed to examine the influence of matrix rigidity on cell growth (Fig. 2A). Cell counting revealed that there was no significant difference in cell growth among all tested TG-Gels on day 1. However, the number of cells in the 3% TG-Gel doubled at a more rapid rate than those in the 6% and 9% TG-Gels after day 1 ($p < 0.001$). The cell proliferation in the 6% and 9% TG-Gels increased exponentially after day 7, and reached a larger cell number than that of the cells encapsulated in 3% TG-Gel ($p < 0.01$), indicating the influence of matrix rigidity on cell growth. CCK-8 and MTT assays were used to further inspect the viability and the mitochondrial activity of the cells in TG-Gels (Fig. 2B). The CCK-8 assay demonstrated the rising trend of the cell viability was corresponded well to the doubling of cell number. The cells in the 3% TG-Gel were initially more viable than those in the 6% and 9% TG-Gels, and yet were less viable on day 14 ($p < 0.001$). The MTT assay revealed the locations of viable cells in TG-Gels, and found that the cells around the periphery of 3% TG-Gel were more active, while the cells located at the center of the 6% and 9% TG-Gels were more viable, as compared with the samples from other groups. Notably, the MTT assay also revealed that the TG-Gel might not limit the nutrients from diffusing into the gel center, as the MTT dye penetrated the center of all TG-Gels under inspection and successfully stained the embedded viable cells.

Besides the differences in cell proliferation and viability, cells may distinguish the difference between soft and rigid matrices by determining the level of tension developed for cell binding, and then respond to the force with counteracting forces. Focal adhesions could be considered for use as force sensors and provide sites at which cells interact with the matrix through anchored actin-microfilament bundles [44,45]. Thus, phalloidin and β1-Integrin staining were performed to visualize the organization of actin filaments (Fig. 2C) and the degree of cell-matrix interactions, respectively (Fig. 2D). Cells encapsulated in the 6% and 9% TG-Gels cultured in the growth medium initially displayed grossly spherical appearance, and some formed clusters at a later time point on day 14. On the contrary, cells embedded in the 3% TG-Gel displayed elongated and branched morphology and established networks on day 14. Phalloidin-staining showed that cells in the 3% TG-Gel exhibited mesh-like or extended actin filaments, whereas dot-like actin-microfilaments with filopodia (indicated by arrows in Fig. 2C) were found in the cells in 6% and 9% TG-Gels. The formation of filopodia allows the cells to engage in various interactions with the matrix [46]. Positive β1-integrin staining further disclosed that the micron-sized cortical protrusions of the cells had entered the surrounding matrix. These protrusions were barely observed in the 3% TG-Gel and were generously present in the 6% and 9% TG-Gels. Both phalloidin and β1-integrin staining suggested that the cells could sense the elasticity of the matrix and counteract the tension exerted on them. In general, a soft matrix favors cell proliferation and actin organization, while a stiff matrix supports cell-matrix interactions.

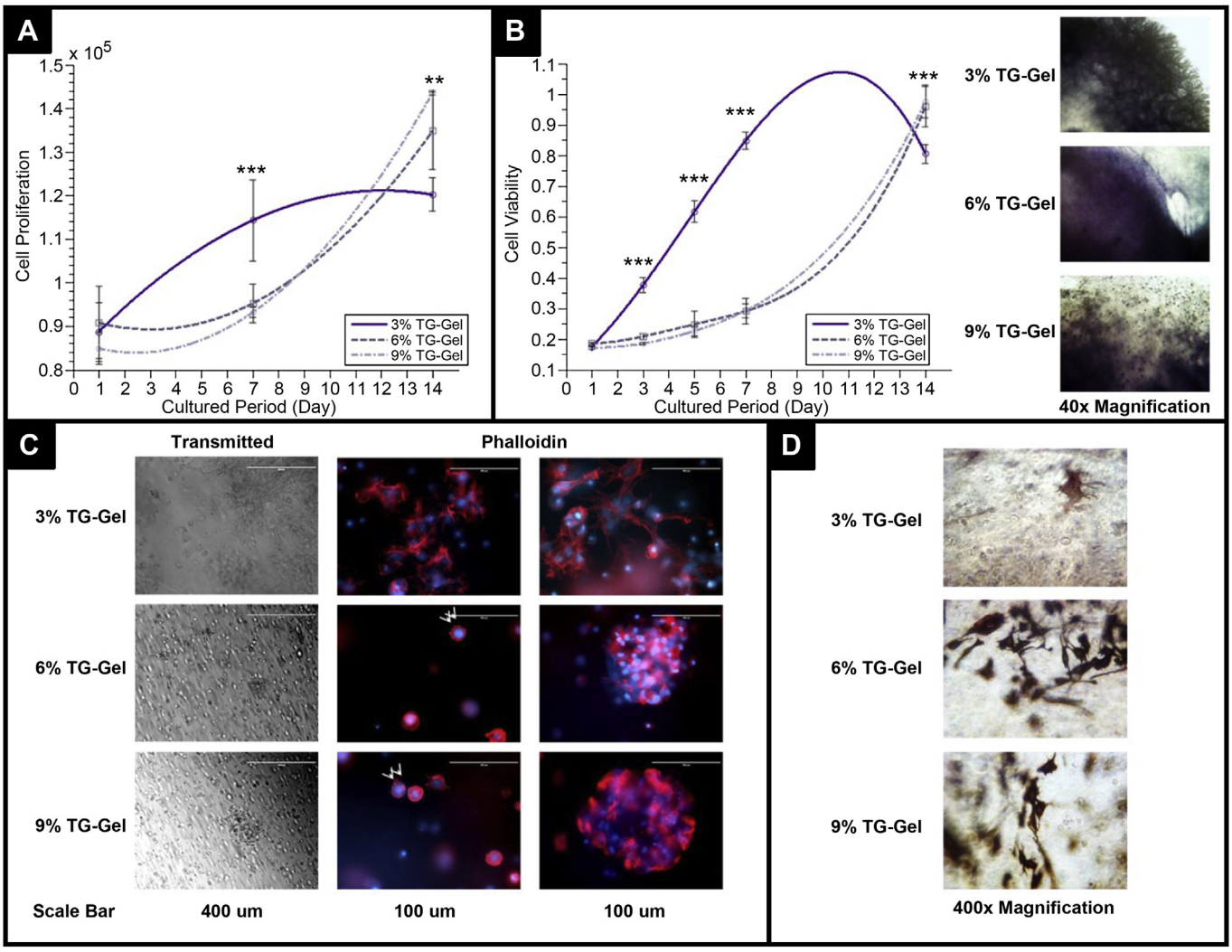

Fig. 2. Influence of matrix rigidity on cellular responses. Cells were encapsulated in 3%, 6% and 9% TG-Gels that cultured in growth medium. (A) Cell counting. The number of cells in the 3% TG-Gel increases at a more rapid rate than those in the 6% and 9% TG-Gels in the beginning. Yet, the cell proliferation in the 6% and 9% TG-Gels increases exponentially after day 7, and has a larger cell number than that of the cells encapsulated in 3% TG-Gel. (B) CCK-8 (left) and MTT (right) assays. CCK-8 assay indicates that the increasing trend of the cell viability is comparable to the cell doubling, where the cells are initially more viable in 3% TG-Gel, but become less active than those in 6% and 9% TG-Gels on day 14 ($p < 0.001$). MTT assay on day 14 reveals the locations of viable cells in TG-Gels. The mitochondrial activity of C2C12s is more viable around the periphery of 3% TG-Gel but more active around the center of 6% and 9% TG-Gels, as compared with the samples from other groups. (C) Phalloidin staining of C2C12s on day 14. Cells embedded in 3% TG-Gel are lengthened in the beginning and established networks on day 14. Yet, cells encapsulated in 6% and 9% TG-Gels appeared grossly spherical and some formed clusters on day 14. The actin filaments of the cells in 3% TG-Gel are in mesh-like or elongated arrangement, whereas dot-like actin actin-microfilaments with filopodia (arrows) are found in 6% and 9% TG-Gels. (D) β1-Integrin staining of cells on day 7. Cell-matrix interactions are more significant in 6% and 9% TG-Gels compared to 3% TG-Gel. Data are mean ± standard deviation, from 4 samples, statistical differences ($^{*}p < 0.05$; $^{**}p < 0.01$; $^{***}p < 0.001$).

3.3. *Influence of matrix stiffness on osteogenic differentiation*

In addition to variations in cell growth and appearance, matrix rigidity may also dictate the cell destiny [43]. Therefore, osteogenic differentiation of C2C12s encapsulated in TG-Gels was evaluated using the Alkaline Phosphatase (ALP) activity assay, ALP and Alizarin red S staining, and by measuring the osteogenic transcription levels (Fig. 3). C2C12s encapsulated in the high-rigidity matrices expressed ALP spontaneously (Fig. 3A). Cells in the 9% TG-Gel expressed the highest ALP activity, followed by the 6% TG-Gel, and the lowest was found in the 3% TG-Gel on day 3 ($p < 0.001$). However, ALP activity of the cells in the 9% TG-Gel decreased from day 5 onward, and the cells in the 6% TG-Gel showed an increase in ALP activity, which was highly expressed on day 14 ($p < 0.001$). Both ALP activity assay and staining demonstrated that the rigid matrix was capable of inducing osteogenic differentiation spontaneously, whereas the soft platform did not facilitate osteogenesis. To better examine the effects of matrix rigidity on osteogenesis, Alizarin red S staining was performed to identify the presence of calcium deposition due to bone nodule formation. The calcium deposition on each substrate in the absence of typical growth factors, such as BMP-2, is shown in Fig. 3B. Alizarin red S staining indicated that the greatest augmentation of the calcium deposition was found in the 9% TG-Gel, followed by the 6% TG-Gel over the predetermined culture period. The C2C12s cultured in 3% TG-Gel demonstrated significantly lower calcium deposition than those embedded in stiff substrates (6% and 9% TG-Gels), further strengthening the hypothesis that the rigidity of matrix itself played a crucial role in cell lineage. Consistently, PCR assay revealed that stiff matrices (6% and 9% TG-Gels) displayed significantly higher osteogenic transcript levels than soft substrate (3% TG-Gel). Furthermore, the 6% TG-Gel showed up-regulated *Osteoblast*, *ALP*,

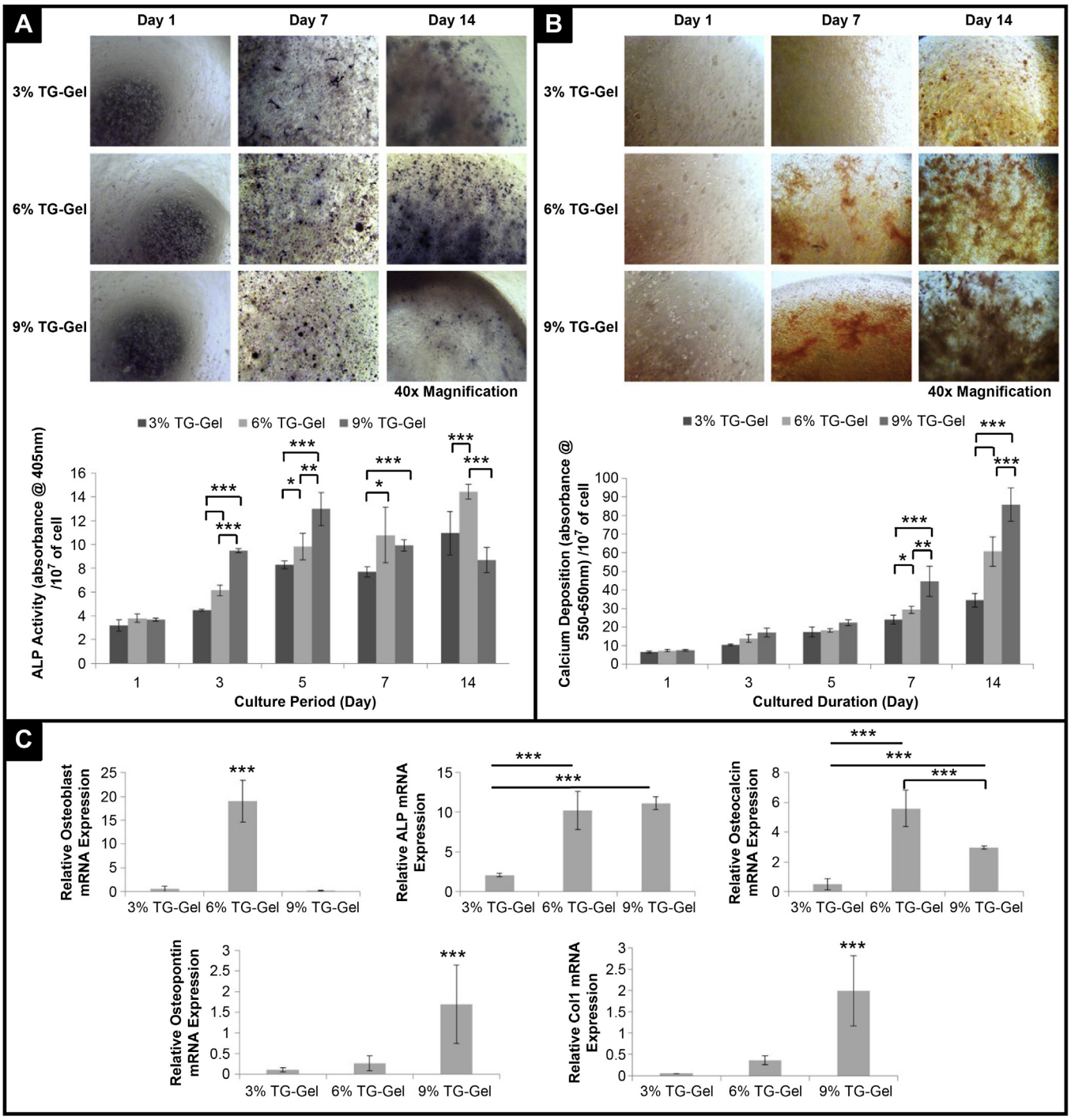

Fig. 3. Matrix rigidity induces spontaneous osteogenesis. Osteogenic differentiation of C2C12s encapsulated in TG-Gel in growth medium was evaluated by ALP activity assay, histochemical staining and osteogenic transcript levels. (A) ALP staining (upper) and activity assay (lower) of C2C12s that encapsulated in 3%, 6% and 9% TG-Gels over cultured period of 1, 3, 5, 7 and 14 days. The ALP expression is spontaneously activated in case of stiff gels (6% and 9% TG-Gels) while relatively low ALP expression is found in case of soft gel (3% TG-Gel). (B) Alizarin Red S staining reveals the calcium deposition of C2C12 cells in 3%, 6% and 9% TG-Gels. The calcium deposition of 6% and 9% TG-Gels are intensifying over the cultured duration while weak calcium deposition is found in 3% TG-Gel. (C) Profile of osteogenic transcript levels on day 14: *Osteoblast*, *ALP*, *Osteocalcin*, *Osteopontin* and *Col1*. Stiff Gels (6% and 9% TG-Gels) exhibit significantly higher osteogenic transcript levels than soft gel (3% TG-Gel). Data are mean ± standard deviation, from 4 samples, statistical differences (*$p < 0.05$; **$p < 0.01$; ***$p < 0.001$).

and *Osteocalcin* expression as compared with the 3% TG-Gel, and the 9% TG-Gel exhibited higher *ALP*, *Osteocalcin*, *Osteopontin* and *Col1* mRNA expression than 3% TG-Gel on day 14 (Fig. 3C). Collectively, a rigid microenvironment is more preferable for cell differentiation into osteoblast-like cells as compared with the soft substrate.

3.4. Influence of BMP-2 and matrix rigidity on cellular responses

BMP-2 was added to our *in vitro* 3-D model to examine the interactions of the mechanical aspects with chemical signals. In 2-D models, BMP-2 has been shown to act as an anti-proliferative agent for a variety of cell lines by activating signaling cascades

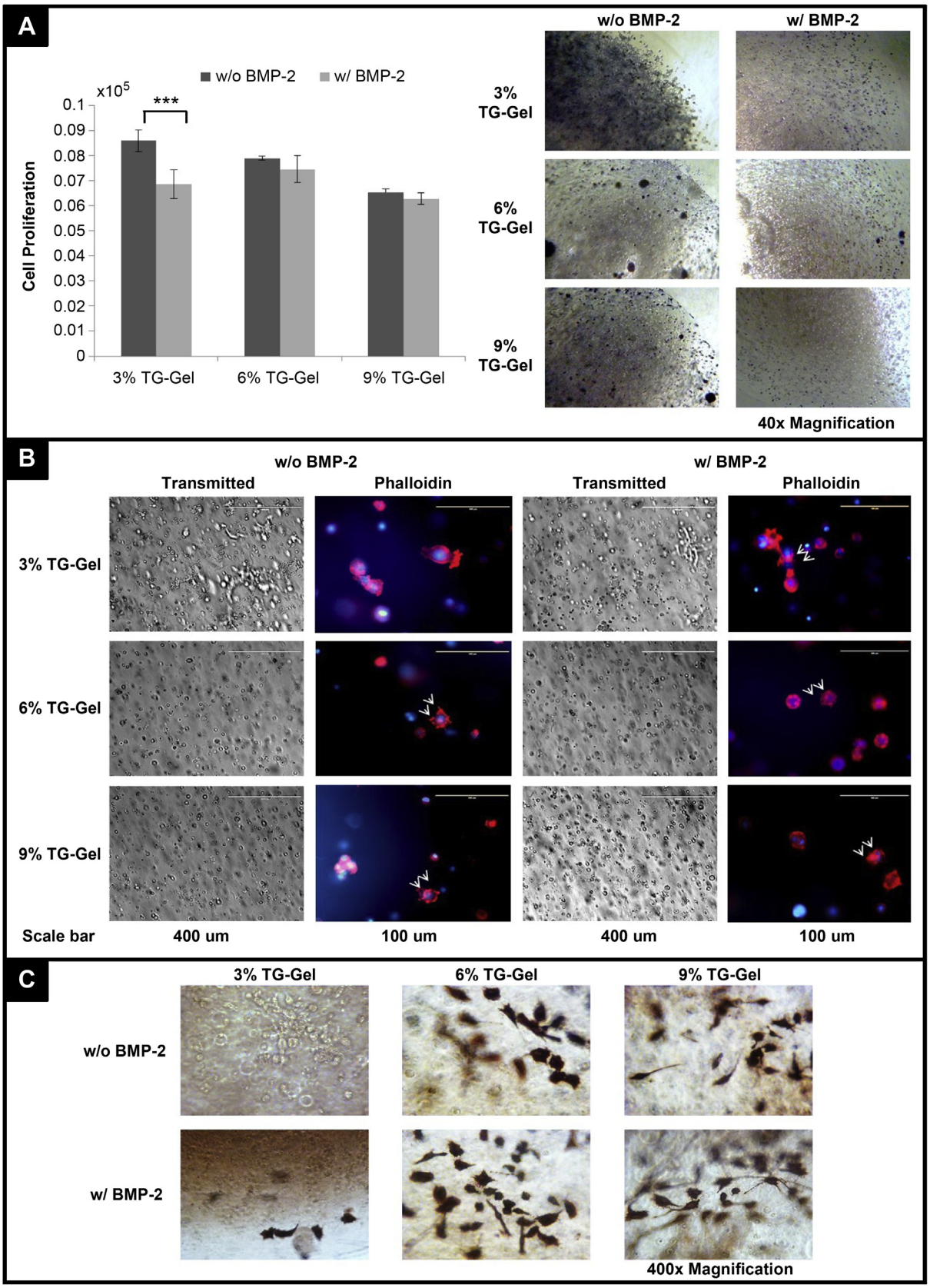

Fig. 4. Influence of BMP-2 in cooperation with TG-Gel on cell responses. Encapsulated C2C12s in TG-Gels were cultured in medium with and without BMP-2 supplement for 5 days. (A) Cell counting (left) and MTT mitochondrial activity assay (right). No statistically difference in the cell proliferation and viability are identified in 6% and 9% TG-Gels in medium with and without BMP-2 supplement, but the growth rate and mitochondrial activity of C2C12s in 3% TG-Gel are substantially reduced with the presence of BMP-2. (B) Phalloidin staining. The appearance of branching cells in 3% TG-Gel in growth medium is reduced with BMP-2 supplement, but cells in the case of stiff matrices (6% and 9% TG-Gels) remained grossly spherical with formation of filopodia (arrows). (C) β1-Integrin staining. The cell-matrix interactions are enhanced by addition of BMP-2, but the interactions are still more significant in 6% and 9% TG-Gels compared to 3% TG-Gel. Data are mean ± standard deviation, from 4 samples, statistical differences (*$p < 0.05$; **$p < 0.01$; ***$p < 0.001$).

that cause cell cycle arrest [47]. To verify this finding in 3-D environment, BMP-2 was included in the model, and cell viability assays were performed. Fig. 4 shows the comparison of cell responses in the growth media with and without BMP-2 supplement. The cell counting, CCK-8 (data not supplemented), and MTT results revealed that BMP-2 significantly constrained the cell growth and the mitochondrial activity of the cells in 3% TG-Gel (Fig. 4A, $p < 0.001$). Yet, no significant impact of BMP-2 supplement on the cell proliferation and viability was identified for the cells encapsulated in 6% and 9% TG-Gels, suggesting that the matrix microenvironment might have restricted cell viability in addition to chemical signals.

To analyze whether BMP-2 could affect the organization of actin cytoskeleton and cell-matrix interactions, C2C12 cells were stimulated with BMP-2 and fixed on day 5, and the filamentous actin was visualized using phalloidin (Fig. 3B) and β1-integrin staining (Fig. 3C). BMP-2 exhibited negligible effects on the gross morphology of the cells in 6% and 9% TG-Gels, while it reduced the appearance of the branching cells in 3% TG-Gel. Phalloidin staining indicated that BMP-2 led to an increase in the formation of dot-like actin filament with filopodia (pointed by arrows in Fig. 3B), suggesting the addictive effects of the growth factor. Additionally, positive β1-integrin staining demonstrated that BMP-2 increased the appearance of filopodia, indicating the enhanced cell-ECM interactions due to BMP-2. Both phalloidin and β1-integrin staining suggested that the addition of BMP-2 did not alter the cell preference to interact with a stiff microenvironment from a softer platform, indicating that the physical properties of microenvironment were equally important as chemical signals for cell characteristics.

3.5. Synergetic effect of BMP-2 and matrix rigidity on osteogenesis

BMP-2 has been widely used in repairing bone defects due to its osteoinductive properties [33,48]. Thus, we added BMP-2 into our TG-Gel models to study its effect on osteogenesis. The additional effect of combining growth factor (i.e. BMP-2) with matrix rigidity for osteogenic differentiation was assessed by examining the ALP activity and mineral deposition (Fig. 5). The ALP activity, calcium deposition, and mRNA expression of TG-Gel in the medium supplied with BMP-2 were normalized with respect to those in the medium without BMP-2 supplementation to demonstrate the up-regulation effect of the former. The cells in all TG-Gels supplemented with BMP-2 expressed significant up-regulated ALP activity and calcium deposition on day 5 as compared with the TG-Gel without BMP-2. Interestingly, the highest rate of osteogenic differentiation induced by BMP-2 was observed in 6% TG-Gel, followed by 9% TG-Gel, and the lowest was found in 3% TG-Gel ($p < 0.001$). Alizarin red S staining revealed that the C2C12 cells cultured in 3% TG-Gel demonstrated significantly lower calcium deposition than the cells embedded in stiff substrates (6% and 9% TG-Gels, $p < 0.001$) did, implying that cells preferred stiffer microenvironment to softer environment for differentiation into osteoblast-like cells. PCR assay further strengthened the assumption that osteoblast-like cells favored stiff matrices (6% and 9% TG-Gels), which displayed apparently higher osteogenic transcript levels than that of the soft matrix (3% TG-Gel). Further, the cells in 6% TG-Gel expressed significantly high bone early markers (i.e., *osteoblast* and *ALP*); whereas 9% TG-Gel showed substantially great late markers (i.e., *ALP*, *osteocalcin*, *osteopontin*, and *Col1*). These findings again demonstrate that the mechanical properties of the ECM were as important as chemical signals in controlling cell lineage. The addition of growth factors did not influence the preference of osteogenic differentiation for occurring in a stiff microenvironment, yet, together with matrix rigidity, affected the regulation of cell responses.

3.6. In vivo overlay model

Animals were euthanized 28 days after subcutaneous injection of 100 μl of various gels over the calvaria. A semi-quantitative histological score scale of the new bone formation and gel contour were evaluated (Fig. 6A). We found that the 3% TG-Gel with and without BMP-2 was dissolved at the injection site after 28 days without the formation of the new bone; however, infiltration of fibroblasts, inflammatory cells, and neovessel invasion were observed. The gel contour of 6% and 9% TG-Gels with and without BMP-2 atop the calvaria were well preserved. There was a small area of new bone formed inside 6% and 9% TG-Gels without BMP-2 that was adjacent to the bony calvaria, revealing TG-Gel as an osteoconductive scaffold. In Contrary, more than 80% of both 6% and 9% TG-Gels with BMP-2 were replaced by bones within the contour of the TG-Gels at 4 weeks after injection (Fig. 6A). In addition, blood vessels were evenly distributed throughout the new bone area, and the edge of the remaining remodeled gel lined up with the osteoblasts, indicating that the rigidity of TG-Gel might not limit the diffusion of nutrients. Fig. 6B presents the cross-sectional view (magnification: 20×) of calvaria injected with 6% TG-Gel and the corresponding image at higher magnification image (magnification: 100×). The full-view image shows bone regeneration at the edge of the gel but fibroblasts were spotted around the center of the gel that was partially dissolved, suggesting that the rigidity of the gel might not be uniform.

4. Discussion

Cells can respond to not only chemical stimuli such as growth factors, cytokines, and hormones [49–52], but also the mechanical properties of the extracellular matrix, such as elastic modulus or rigidity, pore size, porosity, and dynamic mechanical vibration [12,53–58]. Thus, the determination of physical aspects of the matrix is also important for directing the precursor cells into the desired cell fate. More profound understanding about the effects of material rigidity and the cell fate would allow the improvement of the engineered environment for the control of cell fate and regeneration of functional tissue [59,60]. Hence, in this study, we examined the function of precursor cells in differentiating into osteoblast-like cells with the aid of TG-Gels of different rigidities (i.e. 3%, 6%, and 9% TG-Gels). We demonstrated that the adjustment of one or more material parameters would change the cellular responses; soft matrix promoted cell proliferation and actin organization, while stiff matrix supported cell-matrix interactions and osteogenesis. We also evaluated the interactions between BMP-2 and matrix rigidity in a 3-D model. The results indicated that the chemical and physical factors could work synergistically to regulate cell activities. Most importantly, the *in vitro* results obtained from this study were reproducible in our *in vivo* overlay models.

The development of a 3-D material that can support cell survival and allow the investigation of cell responses to the substrate mechanics would be a major breakthrough in tissue engineering. In this study, we demonstrated that the TG-Gel could be a promising biomaterial to overcome many limitations imposed by other substrate systems. Most importantly, the TG-Gel allows the variation of substrate mechanical properties and the degradation profiles in a controllable manner, where a decrease in the gel concentration resulted in the decrease in the gel's yield strength and vice versa (Fig. 1). This result enables the *in vitro* study of the effects of substrate rigidity and cell fate that can simulate the *in vivo* settings as demonstrated in this study. Moreover, the biocompatibility and excellent transparency of the TG-Gel allowed a direct observation under a light microscope, and direct staining to avoid tedious steps such as sectioning and antigen retrieval. Furthermore, the gel

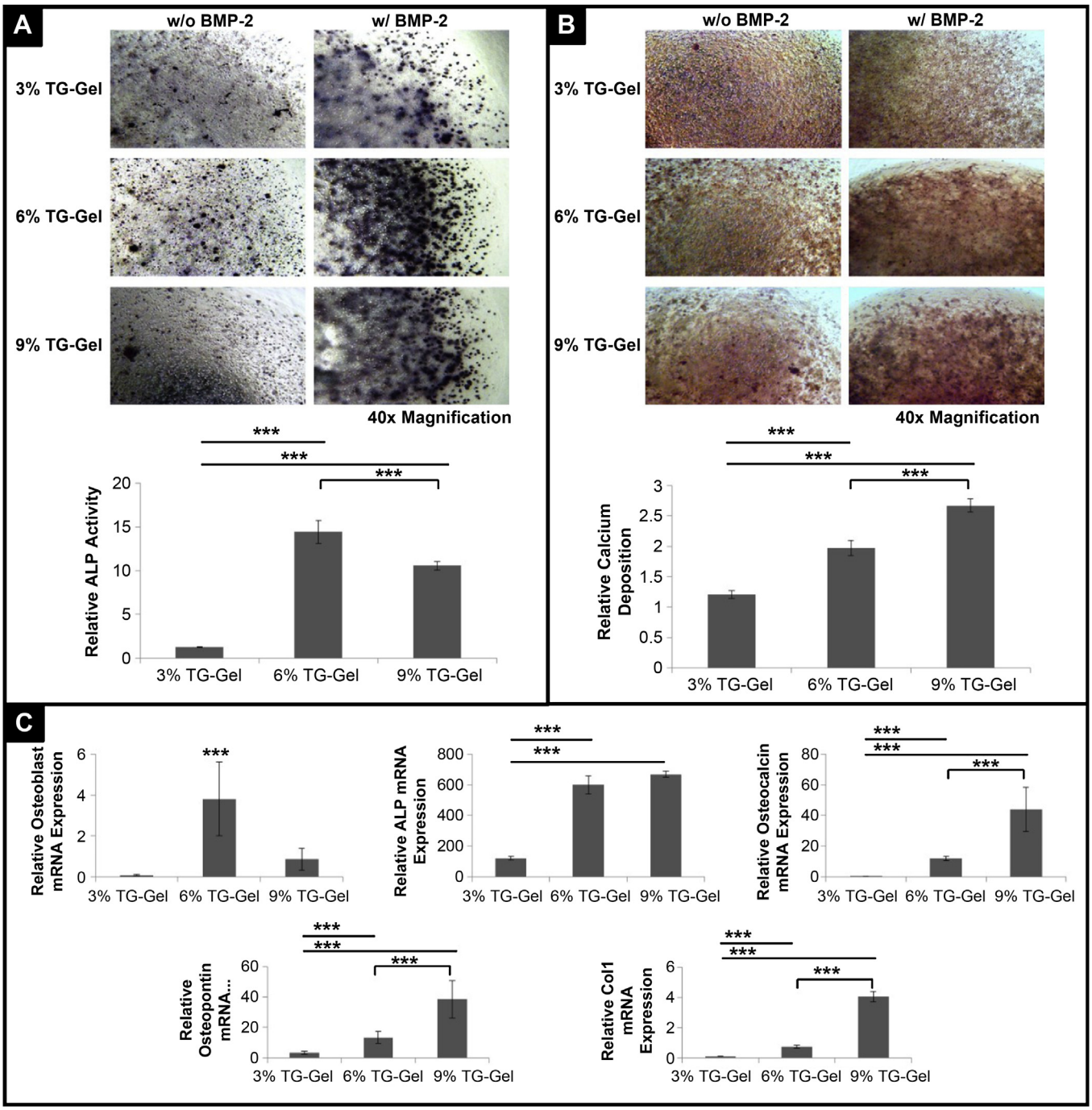

Fig. 5. Effect of BMP-2 and matrix stiffness on osteogenesis. Osteogenic differentiation of C2C12s encapsulated in TG-Gel in medium with and without BMP-2 supplement was evaluated by ALP activity assay, histochemical staining, and osteogenic transcript levels on day 5. The ALP activity, calcium deposition, and mRNA expression of TG-Gel in the medium supplied with BMP-2 were normalized with respect to those in the medium without BMP-2 supplementation. (A) ALP activity as a marker of early osteoblastic differentiation in 3%, 6% and 9% TG-Gels. (B) Alizarin Red S Staining as a marker of late osteoblastic differentiation in 3%, 6% and 9% TG-Gels. (C) Profile of osteogenic transcript levels: *Osteoblast*, *ALP*, *Osteocalcin*, *Osteopontin* and *Col1*. The ALP expression and calcium deposition are up-regulated under all TG-Gels with additional BMP-2 ($p < 0.001$). With BMP-2 supplement, ALP expression is significant higher in 6% TG-Gel while calcium deposition is more up-regulated in 9% TG-Gel, as compared to other groups. Also, osteogenic transcript levels are found significantly higher in stiff gels (6% and 9% TG-Gels) than soft gel (3% TG-Gel). mRNA levels of *osteocalcin*, *osteopontin* and *Col1* of 9% TG-Gel are significant higher than 6% TG-Gel. Data are mean ± standard deviation, from 4 samples, statistical differences (*$p < 0.05$; **$p < 0.01$; ***$p < 0.001$).

provided a stable and durable platform for long-term studies, as we could still vividly see the TG-Gels after 28 days as demonstrated in our *in vivo* models (Fig. 6). One of the concerns about the matrix rigidity is that a high-yield strength material may prevent the diffusion of substances through the substrate. However, in the present study, the decrease in the porosity of the TG-Gel (i.e., high-yield strength material) did not limit the diffusion of nutrients and gas exchange, as the cells were able to survive and function properly within the whole gels as revealed by MTT staining (Figs. 2 and 4). Other staining methods such as ALP and Alizarin red S (Figs. 3 and 5) as well as phalloidin and β1-integrin immunostaining (Figs. 2 and 4) also strengthened the claim that the nutrients and gas could diffuse freely through the gels, regardless of the gel porosity, since the stained colors were clearly shown at the center

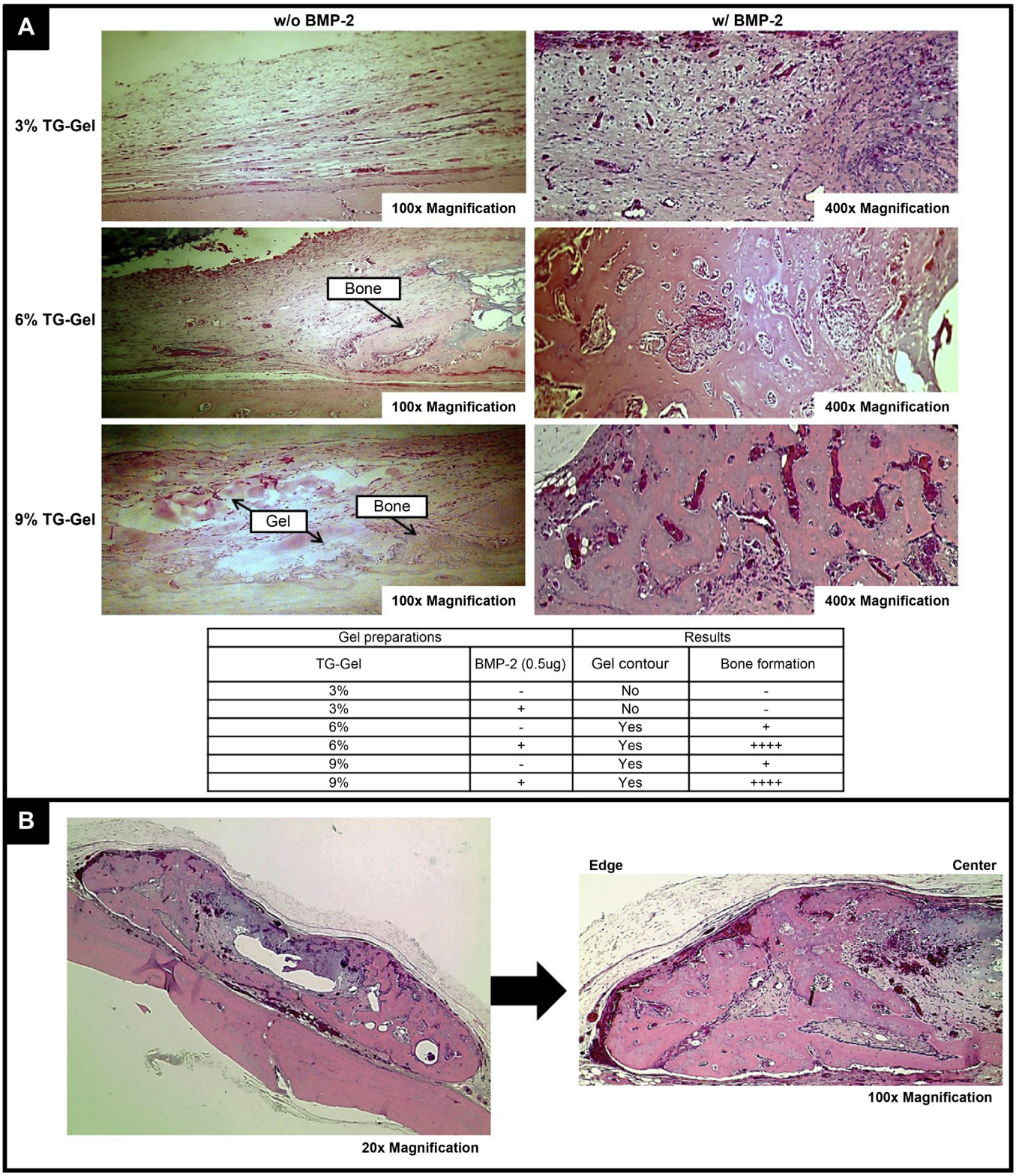

Gel preparations		Results	
TG-Gel	BMP-2 (0.5ug)	Gel contour	Bone formation
3%	-	No	-
3%	+	No	-
6%	-	Yes	+
6%	+	Yes	++++
9%	-	Yes	+
9%	+	Yes	++++

Fig. 6. *In vivo* matrix rigidity model. (A) Comparisons of bone formation with different gel rigidities with and without supplement of BMP-2 in cranial overlay models. After 28 days of subcutaneous injection, explants underwent histology evaluation. H&E was performed and bone formation was evaluated: −: no bone, +: 1–25% bone, ++: 25–50%, +++: 50–75%; ++++: 75–100%. Lower magnification (100× instead of 400×) was taken to demonstrate the location of bone formation for TG-Gels without BMP-2 while higher magnification (400×) was taken to show bone maturation. 3% TG-Gel with and without displays no bone regeneration. There was a small area of new bone formed inside 6% and 9% TG-Gels without BMP-2 that was adjacent to the bony calvaria. Both 400× magnification images of 6% and 9% TG-Gels with BMP-2 show great area of bone formation and maturation. (B) Edge effect model. Lower magnification image (20×) is taken to show the full view of a 6% TG-Gel and its higher magnification image (100×) is taken to better visualize the new tissue formation. Bone formation is found around the edge of the gel while no bone regeneration is observed at the center of the gel.

of the gels. Furthermore, the *in vivo* models demonstrated that the blood vessels were evenly distributed over the new bone areas, implying a good supply of nutrients and gas throughout the gels (Fig. 6). Therefore, the TG-Gel in this study presents a viable model for the study of the influence of substrate rigidity on cell fate and its support to cell survival.

Most of the current studies were performed on coated 2-D surfaces that were not physiologically relevant [25,61,62], and the cells on a coated 2-D surface might not truly present the characteristics of the cells in a more realistic 3-D environment. For example, Park et al. [63] indicated that the cells on a 2-D surface with coated soft collagen showed poorer actin cytoskeleton organization as compared with the cells on a rigid surface. However, we found that the cytoskeleton of the cells in soft 3-D matrix (3% TG-Gel) was well-established with either mesh-like or elongated arrangement, while the cells in stiff 3-D matrices (6% and 9% TG-Gel) formed dot-like actin filaments with filopodia (Fig. 2). This discrepancy might be due to cells are only constrained from the latitudinal direction on a 2-D surface, which they could extend infinitely along the longitudinal direction. On the contrary, the cells seeded in a 3-D environment were constrained from both the longitudinal and latitudinal directions. Thus, the actin filaments of the cells in soft matrix were better developed, as these cells were architecturally better supported by a soft 3-D matrix than by a soft 2-D surface, and were more confined by a stiff 3-D platform than by a rigid 2-D surface. Because 3-D environments provide an additional dimension for external mechanical inputs and for cell adhesion, they can dramatically affect integrin ligation, cell contraction, and associated intracellular signaling [64,65]. Hence, the cells on a 2-D platform are less mechanosensitive than those in the 3-D environment.

Cells can respond to various environmental signals within the extracellular matrix (ECM), deviate from their original cellular structures, and eventually alter their functionalities [66]. Hence, cells existing in different materials might not show identical behaviors. We found that osteogenic differentiation primarily occurred in the 6% and 9% TG-Gels (13.51 $\pm$ 2.13 kPa and 32.32 $\pm$ 1.9 kPa, respectively), and this was consistent with the finding of Huebsch et al. [28], who studied cell differentiation in 3-D alginate and agarose that were covalently coupled with the integrin-binding peptide. In addition to osteogenic-differentiation, the cytoskeleton organization in stiff microenvironments (6% and 9% TG-Gels) was as determined by Huebsch et al. [28], who found that the cells showed grossly spherical appearance with micron-sized cortical protrusions. Although Huebsch et al. [28] claimed no strong correlation existing between cell morphology and cell fate, we observed that the cells in the soft matrix (3% TG-Gel) exhibited a branching form with less prominent osteoblastic polygonal morphology and osteogenic marker than those of the cells in the stiff microenvironments (6% and 9% TG-Gels). This might be due to the fact that the substrate rigidities adopted in their study varied from 2.5 to 100 kPa, whereas the yield strength of the 3% TG-Gel in our study, where branching morphology was observed, was less than 2.5 kPa. Other material properties such as porosity, pore size, and cells adhesion site might contribute to the discrepancies in the findings. Perhaps, the yield strength and porosity of the TG-Gels that were measured prior to the cell addition may not be representative of the final values towards the end of the study, due to the possible degradation of TG-Gels via the enzymatic activities of collagenase and MMPs [31]. Moreover, the endogenous extracellular matrix assembly and deposition might occur, as the *collagen I* (*Col I*) expression in the matrices became significant and promoted osteogenesis (Figs. 3 and 5). The competition of cell diffusion and convection with cell consumption or production leads to uneven distribution of porosity across the gels observed in our *in vivo* model, where the edge of the gel remained intact, while the center degraded after 28 days of study (Fig. 6B). Therefore, further evaluations on the dynamic changes in mechanical properties of the matrices are necessary for creating the ideal carrier for cell regeneration.

The state-of-the-art regenerative medicine envisages the utilization of growth factors coupled with scaffolds or immobilized on biomaterials [67–69] for the accelerated tissue regeneration. Moreover, the usage of BMP-2 in carriers or ex vivo progenitor cells with BMP-2 is subject to critical evaluation [70–72]. Thus, BMP-2 was added into our models to study the effects of chemical stimuli and matrix rigidity on bone regeneration. Although Wen et al. [47] discovered that BMP-2 showed inhibitory effect on cell proliferation on 2-D platform without taking matrix rigidity into account, we found that BMP-2 reduced the cell proliferation and viability and altered the cell appearance in only soft matrix (3% TG-Gel), and very little or no effect of BMP-2 was found in the case of stiff matrices (6% and 9% TG-Gel). This might be due to the stiffness of the matrices (6% and 9% TG-Gel) confined the cell characteristics to the baseline threshold and further enhanced the significance of the mechanical aspects. Rapid progress of osteogenesis was observed in stiffer substrates, particularly at 9% TG-Gel. 9% TG-Gel with and without BMP-2 supplement exhibited highest calcium deposition and late markers of osteogenic differentiation in our *in vitro* studies, while ALP activity and early markers of osteogenic differentiation were more profound in 6% TG-Gel (Figs. 3 and 5). This might be due to the matrix rigidity of 9% TG-Gel ($E \approx 32$ kPa) mimics the native tissue environment ($E \approx 25$–40 kPa) [12], where cells are able to sense the rigidity and differentiate directly to the appropriate cell type. Depending upon the length of time, cells encapsulated in 6% TG-Gel with lower elasticity ($E \approx 14$ kPa) may assemble and deposit their own matrix to match the ideal bone microenvironment. Thus, the cells in 6% TG-Gel differentiated to osteoblast-like cells at the later time point. Consistently, 9% TG-Gels with BMP-2 were found to induce more bone formation and maturation in our *in vivo* model compared to 6% TG-Gels with BMP-2 (Fig. 6). Both *in vitro* and *in vivo* results further substantiate the crucial role of physical properties of ECM in deciding cell fate. Interestingly, the addition of BMP-2 into our models did not alter the finding that osteogenic differentiation occurred primarily in stiffer 3-D settings (Figs. 3 and 5). Yet, the addition of BMP-2 into our model significantly intensified osteogenesis in stiff matrices (6% and 9% TG-Gels) as demonstrated in both *in vitro* and *in vivo* models (Figs. 5 and 6). Hence, both physical and chemical factors are equivalently vital and can synergistically regulate the cell responses.

5. Conclusions

It has become evident that adjuvant materials for repairing genetic or accidental bone defects need to mimic the physiological environment to support and control the release of growth factors to amplify the regenerative capacity. Our inexpensive and scalable TG-Gel system enlightens a niche area for regenerative medicine, as it can be integrated either as a testing model or as a potential carrier for cells and growth factors. The cell delivery by a protective gel may enhance the cell survival and stimulate the function of endogenous stem cells. Furthermore, the loading of diffusible cytokines and growth factors into the carrier may also promote the mobility of endogenous cells that are involved in the cell repairmen, enhancement of cell survival, stimulation of cell self-renewal, and expansion of the transplanted cells. The spatial and temporal control of these features would enhance their usability in tissue regeneration, improve tissue function, and overcome the adverse effects of diseases or aging. Certainly, a platform with

mechanical properties variable in gradient may be designed to compensate the drawback due to uneven pore distribution.

References

[1] Liedert A, Kaspar D, Augat P, Ignatius A, Claes L. Mechanobiology of bone tissue and bone cells. In: Kamkin A, Kiseleva I, editors. Mechanosensitivity in cells and tissues. Moscow: Academia; 2005.
[2] Aspenberg P, Goodman S, Toksvig-Larsen S, Ryd L, Albrektsson T. Intermittent micromotion inhibits bone ingrowth: titanium implants in rabbits. Acta Orthop 1992;63:141–5.
[3] Claes L, Wilke H, Augat P, Rübenacker S, Margevicius K. Effect of dynamization on gap healing of diaphyseal fractures under external fixation. Clin Biomech (Bristol, Avon) 1995;10:227–34.
[4] Kenwright J, Goodship AE. Controlled mechanical stimulation in the treatment of tibial fractures. Clin Orthop Relat Res 1989;241:36–47.
[5] Goodship AE, Cunningham JL, Kenwright J. Strain rate and timing of stimulation in mechanical modulation of fracture healing. Clin Orthop Relat Res 1998;355:S105–15.
[6] Campbell GR, Campbell JH. Smooth muscle phenotypic changes in arterial wall homeostasis: implications for the pathogenesis of atherosclerosis. Exp Mol Pathol 1985;42:139–62.
[7] Glukhova MA, Koteliansky VE. Integrins, cytoskeletal and extracellular matrix proteins in developing smooth muscle cells of human aorta. In: Schwartz SM, Mechams RP, editors. The vascular smooth muscle cell. London: Academic Press; 1995. pp. 37–9.
[8] Stedman H, Sweeney H, Shrager J, Maguire H, Panettieri R, Petrof B, et al. The mdx mouse diaphragm reproduces the degenerative changes of Duchenne muscular dystrophy. Nature 1991;352:536–9.
[9] Harrison DG. Cellular and molecular mechanisms of endothelial cell dysfunction. J Clin Invest 1997;100:2153.
[10] Chen CS, Mrksich M, Huang S, Whitesides GM, Ingber DE. Geometric control of cell life and death. Science 1997;276:1425–8.
[11] Yeung T, Georges PC, Flanagan LA, Marg B, Ortiz M, Funaki M, et al. Effects of substrate stiffness on cell morphology, cytoskeletal structure, and adhesion. Cell Motil Cytoskeleton 2005;60:24–34.
[12] Engler AJ, Sen S, Sweeney HL, Discher DE. Matrix elasticity directs stem cell lineage specification. Cell 2006;126:677–89.
[13] Hu X, Park S-H, Gil ES, Xia X-X, Weiss AS, Kaplan DL. The influence of elasticity and surface roughness on myogenic and osteogenic-differentiation of cells on silk-elastin biomaterials. Biomaterials 2011;32:8979–89.
[14] EGB K, Ingegneria Genetica C. Mechanotransduction across the cell surface and through the cytoskeleton. Science 1993;260:21.
[15] Ingber DE. Cellular tensegrity: defining new rules of biological design that govern the cytoskeleton. J Cell Sci 1993;104:613–27.
[16] Girard PR, Nerem RM. Shear stress modulates endothelial cell morphology and F-actin organization through the regulation of focal adhesion-associated proteins. J Cell Physiol 1995;163:179–93.
[17] Davies PF. Flow-mediated endothelial mechanotransduction. Physiol Rev 1995;75:519.
[18] Choquet D, Felsenfeld DP, Sheetz MP. Extracellular matrix rigidity causes strengthening of integrin–cytoskeleton linkages. Cell 1997;88:39–48.
[19] Wang N, Tolić-Nµrrelykke IM, Chen J, Mijailovich SM, Butler JP, Fredberg JJ, et al. Cell prestress. I. Stiffness and prestress are closely associated in adherent contractile cells. Am J Physiol Cell Physiol 2002;282:C606–16.
[20] Grinnell F, Ho C-H, Lin Y-C, Skuta G. Differences in the regulation of fibroblast contraction of floating versus stressed collagen matrices. J Biol Chem 1999;274:918–23.
[21] Zaman MH, Kamm RD, Matsudaira P, Lauffenburger DA. Computational model for cell migration in three-dimensional matrices. Biophys J 2005;89:1389–97.
[22] Lutolf M, Lauer-Fields J, Schmoekel H, Metters A, Weber F, Fields G, et al. Synthetic matrix metalloproteinase-sensitive hydrogels for the conduction of tissue regeneration: engineering cell-invasion characteristics. Proc Natl Acad Sci U S A 2003;100:5413–8.
[23] Lo CM, Wang HB, Dembo M, Yl Wang. Cell movement is guided by the rigidity of the substrate. Biophys J 2000;79:144–52.
[24] Peyton SR, Putnam AJ. Extracellular matrix rigidity governs smooth muscle cell motility in a biphasic fashion. J Cell Physiol 2005;204:198–209.
[25] Cukierman E, Pankov R, Stevens DR, Yamada KM. Taking cell-matrix adhesions to the third dimension. Science 2001;294:1708–12.
[26] Griffith LG, Swartz MA. Capturing complex 3D tissue physiology in vitro. Nat Rev Mol Cell Biol 2006;7:211–24.
[27] Pek YS, Wan AC, Ying JY. The effect of matrix stiffness on mesenchymal stem cell differentiation in a 3D thixotropic gel. Biomaterials 2010;31:385–91.
[28] Huebsch N, Arany PR, Mao AS, Shvartsman D, Ali OA, Bencherif SA, et al. Harnessing traction-mediated manipulation of the cell/matrix interface to control stem-cell fate. Nat Mater 2010;9:518–26.
[29] Haraguchi K. Synthesis and properties of soft nanocomposite materials with novel organic/inorganic network structures. Polym J 2011;43:223–41.
[30] Chang C-W, van Spreeuwel A, Zhang C, Varghese S. PEG/clay nanocomposite hydrogel: a mechanically robust tissue engineering scaffold. Soft Matter 2010;6:5157–64.
[31] Fang J, Yang Z, Tan S, Tayag C, Nimni ME, Urata M, et al. Injectable gel graft for bone defect repair. Regen Med 2014;9:41–51.
[32] Baylink DJ, Finkelman RD, Mohan S. Growth factors to stimulate bone formation. J Bone Miner Res 1993;8:S565–72.
[33] Tsuji KAB, Harfe BD, Cox K, Kakar S, Gerstenfeld L, Einhorn T, et al. BMP-2 activity, although dispensable for bone formation, is required for the initiation of fracture healing. Nat Genet 2006;38:1424–9.
[34] Kuwahara JYF K, Yang Z, Han B. Enzymatic crosslinking and degradation of gelatin as a switch for bone morphogenetic protein-2 activity. Tissue Eng 2011;17:2955–64.
[35] Kuwahara K, Yang Z, Slack GC, Nimni ME, Han B. Cell delivery using an injectable and adhesive transglutaminase–gelatin gel. Tissue Eng 2009;16:609–18.
[36] Dinnella C, Gargaro MT, Rossano R, Monteleone E. Spectrophotometric assay using o-phtaldialdehyde for the determination of transglutaminase activity on casein. Food Chem 2002;78:363–8.
[37] Bradford MM. A rapid and sensitive method for the quantitation of microgram quantities of protein utilizing the principle of protein-dye binding. Anal Biochem 1976;72:248–54.
[38] Guan J, Fujimoto KL, Sacks MS, Wagner WR. Preparation and characterization of highly porous, biodegradable polyurethane scaffolds for soft tissue applications. Biomaterials 2005;26:3961–71.
[39] Mosmann T. Rapid colorimetric assay for cellular growth and survival: application to proliferation and cytotoxicity assays. J Immunol Methods 1983;65:55–63.
[40] Han B, Tang B, Nimni ME. Quantitative and sensitive in vitro assay for osteoinductive activity of demineralized bone matrix. J Orthop Res 2003;21:648–54.
[41] Jiang G, Huang AH, Cai Y, Tanase M, Sheetz MP. Rigidity sensing at the leading edge through αvβ3 integrins and RPTPα. Biophys J 2006;90:1804–9.
[42] Chomczynski P, Sacchi N. Single-step method of RNA isolation by acid guanidinium thiocyanate-phenol-chloroform extraction. Anal Biochem 1987;162:156–9.
[43] Huang S, Ingber DE. The structural and mechanical complexity of cell-growth control. Nat Cell Biol 1999;1:E131–8.
[44] McBeath R, Pirone DM, Nelson CM, Bhadriraju K, Chen CS. Cell shape, cytoskeletal tension, and RhoA regulate stem cell lineage commitment. Dev Cell 2004;6:483–95.
[45] Katz B-Z, Zamir E, Bershadsky A, Kam Z, Yamada KM, Geiger B. Physical state of the extracellular matrix regulates the structure and molecular composition of cell-matrix adhesions. Mol Biol Cell 2000;11:1047–60.
[46] Giancotti FG, Ruoslahti E. Integrin signaling. Science 1999;285:1028–33.
[47] Wen X-Z, Miyake S, Akiyama Y, Yuasa Y. BMP-2 modulates the proliferation and differentiation of normal and cancerous gastric cells. Biochem Biophys Res Commun 2004;316:100–6.
[48] McKay WF, Peckham SM, Badura JM. A comprehensive clinical review of recombinant human bone morphogenetic protein-2 (INFUSE® Bone Graft). Int Orthop 2007;31:729–34.
[49] Bax DV, Rodgers UR, Bilek MM, Weiss AS. Cell adhesion to tropoelastin is mediated via the C-terminal GRKRK motif and integrin αVβ3. J Biol Chem 2009;284:28616–23.
[50] Taddese S, Weiss AS, Jahreis G, Neubert RH, Schmelzer CE. *In vitro* degradation of human tropoelastin by MMP-12 and the generation of matrikines from domain 24. Matrix Biol 2009;28:84–91.
[51] Getie M, Schmelzer C, Neubert R. Characterization of peptides resulting from digestion of human skin elastin with elastase. Proteins 2005;61:649–57.
[52] Phillips JE, Petrie TA, Creighton FP, García AJ. Human mesenchymal stem cell differentiation on self-assembled monolayers presenting different surface chemistries. Acta Biomater 2010;6:12–20.
[53] Nemir S, West JL. Synthetic materials in the study of cell response to substrate rigidity. Ann Biomed Eng 2010;38:2–20.
[54] Holst J, Watson S, Lord MS, Eamegdool SS, Bax DV, Nivison-Smith LB, et al. Substrate elasticity provides mechanical signals for the expansion of hemopoietic stem and progenitor cells. Nat Biotechnol 2010;28:1123–8.
[55] Rowlands AS, George PA, Cooper-White JJ. Directing osteogenic and myogenic differentiation of MSCs: interplay of stiffness and adhesive ligand presentation. Am J Physiol Cell Physiol 2008;295:C1037–44.
[56] Hamilton DW, Maul TM, Vorp DA. Characterization of the response of bone marrow-derived progenitor cells to cyclic strain: implications for vascular tissue-engineering applications. Tissue Eng 2004;10:361–9.
[57] You M-H, Kwak MK, Kim D-H, Kim K, Levchenko A, Kim D-Y, et al. Synergistically enhanced osteogenic differentiation of human mesenchymal stem cells by culture on nanostructured surfaces with induction media. Biomacromolecules 2010;11:1856–62.
[58] Fu J, Wang Y-K, Yang MT, Desai RA, Yu X, Liu Z, et al. Mechanical regulation of cell function with geometrically modulated elastomeric substrates. Nat Methods 2010;7:733–6.
[59] Silva EA, Kim E-S, Kong HJ, Mooney DJ. Material-based deployment enhances efficacy of endothelial progenitor cells. Proc Natl Acad Sci U S A 2008;105:14347–52.
[60] Ali OA, Huebsch N, Cao L, Dranoff G, Mooney DJ. Infection-mimicking materials to program dendritic cells in situ. Nat Mater 2009;8:151–8.
[61] Fischbach C, Kong HJ, Hsiong SX, Evangelista MB, Yuen W, Mooney DJ. Cancer cell angiogenic capability is regulated by 3D culture and integrin engagement. Proc Natl Acad Sci U S A 2009;106:399–404.

[62] Hsiong SX, Boontheekul T, Huebsch N, Mooney DJ. Cyclic arginine-glycine-aspartate peptides enhance three-dimensional stem cell osteogenic differentiation. Tissue Eng 2008;15:263–72.
[63] Park JS, Huang NF, Kurpinski KT, Patel S, Hsu S, Li S. Mechanobiology of mesenchymal stem cells and their use in cardiovascular repair. Front Biosci 2007;12:5098–116.
[64] Knight B, Laukaitis C, Akhtar N, Hotchin NA, Edlund M, Horwitz AR. Visualizing muscle cell migration *in situ*. Curr Biol 2000;10:576–85.
[65] Roskelley C, Desprez P, Bissell M. Extracellular matrix-dependent tissue-specific gene expression in mammary epithelial cells requires both physical and biochemical signal transduction. Proc Natl Acad Sci U S A 1994;91:12378–82.
[66] García AJ. Get a grip: integrins in cell–biomaterial interactions. Biomaterials 2005;26:7525–9.
[67] Bessa PC, Casal M, Reis R. Bone morphogenetic proteins in tissue engineering: the road from laboratory to clinic, part II (BMP delivery). J Tissue Eng Regen Med 2008;2:81–96.
[68] Senta H, Park H, Bergeron E, Drevelle O, Fong D, Leblanc E, et al. Cell responses to bone morphogenetic proteins and peptides derived from them: biomedical applications and limitations. Cytokine Growth Factor Rev 2009;20:213–22.
[69] Kempen DH, Lu L, Heijink A, Hefferan TE, Creemers LB, Maran A, et al. Effect of local sequential VEGF and BMP-2 delivery on ectopic and orthotopic bone regeneration. Biomaterials 2009;30:2816–25.
[70] Li RH, Wozney JM. Delivering on the promise of bone morphogenetic proteins. Trends Biotechnol 2001;19:255–65.
[71] Dragoo JL, Choi JY, Lieberman JR, Huang J, Zuk PA, Zhang J, et al. Bone induction by BMP-2 transduced stem cells derived from human fat. J Orthop Res 2003;21:622–9.
[72] Peterson B, Zhang J, Iglesias R, Kabo M, Hedrick M, Benhaim P, et al. Healing of critically sized femoral defects, using genetically modified mesenchymal stem cells from human adipose tissue. Tissue Eng 2005;11:120–9.